

H I studies of eXtremely Metal Deficient galaxies – II. Giant Metrewave Radio Telescope observations of SBS 1129+576

Ekta,^{1*} Jayaram N. Chengalur,^{1*} Simon A. Pustilnik^{2*}

¹ National Centre for Radio Astrophysics, Post Bag 3, Ganeshkhind, Pune 411 007, India

² Special Astrophysical Observatory of RAS, Nizhnij Arkhiz, Karachai-Circasia 369167, Russia

Accepted 2006 July 31. Received 2006 July 20; in original form 2006 May 16

ABSTRACT

We present Giant Metrewave Radio Telescope H I observations of an eXtremely Metal Deficient galaxy SBS 1129+576. SBS 1129+576 has a weighted mean oxygen abundance of $12 + \log (\text{O}/\text{H}) = 7.41 \pm 0.07$, or 1/18 of the solar value. Our H I observations show that the galaxy is strongly interacting with a companion (projected separation ~ 27 kpc) galaxy, SBS 1129+577. H I emission from a third, smaller galaxy, SDSS J113227.68+572142.3, is also present in the data cube. We study the H I morphology and kinematics of this small group at angular resolutions ranging from ~ 40 to 8 arcsec. The low-resolution map shows a bridge of emission connecting the two larger galaxies and a large one-armed spiral distortion of the disc of SBS 1129+577. We measure H I masses of $\sim 4.2 \times 10^8$, $\sim 2.7 \times 10^9$, and $\sim 2.1 \times 10^8 M_{\odot}$ for SBS 1129+576, SBS 1129+577 and the gas in the bridge, respectively. Assuming that most of the bridge gas originally came from SBS 1129+576, approximately one-third of its original gas mass has been stripped off. The third smaller galaxy has an H I mass of ($M_{\text{HI}} \sim 1.1 \times 10^7 M_{\odot}$) and does not show any sign of interaction with the other two galaxies. The higher-resolution maps show that SBS 1129+577 has a central bar and a ring surrounding the bar; there is also a hint of an integral-shaped warp in SBS 1129+576. All these features are very likely to have been induced by the tidal interaction. In both SBS 1129+576 and SBS 1129+577, there is, in general, a good correspondence between regions with high H I column density and those with ongoing star formation. The two brightest H II regions in SBS 1129+576 have (inclination-corrected) gas column densities of $\sim 1.6 \times 10^{21}$ and $\sim 1.8 \times 10^{21}$ atoms cm^{-2} , respectively. The inclination-corrected H I column density near the H II regions in SBS 1129+577 is generally above $\sim 2.0 \times 10^{21}$ atoms cm^{-2} . These values are close to the threshold density for star formation observed in other blue compact galaxies. In contrast to SBS 1129+576 and SBS 1129+577 which are very gas-rich, the third member of this group, SDSS J113227.68+572142.3, is gas-poor.

Key words: galaxies: dwarf – galaxies: evolution – galaxies: individual: SBS 1129+576 – galaxies: individual: SBS 1129+577 – galaxies: individual: SDSS J113227.68+572142.3 – galaxies: interactions – galaxies: kinematics and dynamics – radio lines: galaxies

1 INTRODUCTION

A very small fraction of low-mass, gas-rich galaxies have very low observed interstellar medium (ISM) metallicities, $12 + \log (\text{O}/\text{H}) \leq 7.65$. About 50 such galaxies are now known (see e.g. the review by Kunth & Östlin 2000)

and are termed here as eXtremely Metal Deficient (XMD) galaxies. A few XMD galaxies, for example, I Zw 18 and SBS 0335–052 E and W, where there is no evidence for an old stellar population, are considered as good candidates for young galaxies in the local Universe. In general, however, old stellar populations have been found in most (of the as of yet small numbers) of well-studied XMD galaxies. Despite the presence of an older stellar population, the

* ekta@ncra.tifr.res.in, chengalu@ncra.tifr.res.in, sap@sao.ru

very low ISM metallicities of XMDs indicate that they are relatively unevolved systems. Further evidence for their relatively unevolved status comes from the fact that they are very gas rich; neutral hydrogen is often the dominant baryonic component in these galaxies. The study of the neutral hydrogen content, distribution and kinematics is hence important in understanding this small, but interesting subclass of dwarf galaxies. As the best local analogues of young low-mass galaxies in the high-redshift Universe, detailed studies of the connections between the gas distribution, kinematics and star formation in these galaxies could provide useful input into models of galaxy formation and evolution. A systematic, H I survey of 22 XMD galaxies was conducted at the Nançay Radio Telescope (NRT) by Pustilnik & Martin (2006, Paper I). This survey increased the number of XMD galaxies with available integrated H I parameters by almost a factor of 2 (earlier surveys were done by e.g. Thuan et al. 1999). Follow-up interferometric observations of a subsample of the galaxies observed at the NRT are being done using the Giant Metrewave Radio Telescope (GMRT). SBS 1129+576, the subject of this paper, is the first object from this subsample.

SBS 1129+576 is a very metal-poor (with weighted mean oxygen abundance $12 + \log(O/H) = 7.41 \pm 0.07$; Guseva et al. 2003) nearby blue compact galaxy (BCG). It was discovered as part of the Second Byurakan Survey (SBS) (Markarian and Stepanian 1983; Lipovetsky et al. 1988). Pustilnik et al. (2001b) measure $M_B \sim 16.50$ mag for this galaxy. Guseva et al. (2003) present *V*- and *I*-band CCD images as well as spectroscopic data for this galaxy. The CCD images show the galaxy to contain a chain of compact H II regions within an elongated low surface brightness (LSB) envelope. The H II regions and the LSB component both are bluer than typical for dwarf irregular or even blue compact dwarf (BCD) galaxies. The blue colour and the very low metallicity of SBS 1129+576 both are indicative of a relatively young age for the dominant stellar population. However, as is generally the case with very low metallicity galaxies, the spectroscopic and photometric data do not allow one to rule out models in which the galaxy contains stellar populations as old as 10 Gyr, albeit with the majority of the current luminosity coming from a much younger (~ 100 Myr) population.

Thuan et al. (1999) presented NRT H I data for SBS 1129+576. The measured heliocentric velocity is 1566 ± 2 km s⁻¹, which corresponds to a distance of 26.3 Mpc (after correction for Virgocentric infall). Thuan et al. (1999) noted the possibility of confusion with a nearby dwarf irregular galaxy, SBS 1129+577 (MCG+10-17-010). Pustilnik et al. (2001a) suggested that interaction with this companion probably triggered starburst in SBS 1129+576, whereas Petrosian et al. (2002) noted that SBS 1129+576 has a peculiar disturbed morphology and classified it as a ‘merger’.

We present here GMRT H I 21-cm observations of emission from the SBS 1129+576/577 pair. The rest of this paper is divided as follows. In Section 2, the observations and data reduction are described, while the results of the observations are described in Section 3. In Section 4, we compare SBS 1129+576 with the other very metal-poor galaxies, and Section 5 provides a summary of our results.

Table 1. Parameters of the observations using the GMRT

Date of observations	2004 February 12
Field centre RA(J2000)	11 ^h 32 ^m 02 ^s .507
Field centre Dec.(J2000)	57° 24′ 39″.960
The velocity at the band centre	1566 km s ⁻¹
Time on source	7 h
Number of channels	128
Channel separation	3.3 km s ⁻¹
Synthesized beams (FWHM in arcsec ²)	42 × 40, 17 × 14, 8 × 7
rms noise (mJy beam ⁻¹)	1.6, 1.1, 1.0

2 OBSERVATIONS AND DATA REDUCTION

The GMRT observations, conducted on 2004 February 12 (see Table 1) had a total on-source time of ~ 7 h. The observations used a total bandwidth of 2.0 MHz (~ 425 km s⁻¹) centred at 1413.0 MHz. The FX correlator provided 128 spectral channels, that is, a spectral resolution of ~ 15.6 kHz (~ 3.3 km s⁻¹). Flux and bandpass calibration was done using short observations of 3C 48 and 3C 286, while phase calibration was done using either one of the VLA calibrator sources 1035+564 or 1219+584. After flagging out bad-visibility points, flux and phase calibration was done for a single spectral channel. This calibration was applied to the original multichannel file, after which bandpass calibration was done. Finally, flux-, phase- and bandpass-calibrated visibilities for the target source were split out into a separate uv-file using the task SPLIT. Continuum emission was subtracted from the visibilities using the task UVSUB. The GMRT has a hybrid configuration which allows images at a range of resolutions to be made from data from a single observing run. Spectral image cubes were hence made at several angular resolutions ranging from ~ 40 to ~ 8 arcsec. Integrated H I emission as well as the H I velocity field were derived using the task MOMNT.

3 RESULTS OF THE OBSERVATIONS

3.1 Continuum emission

No continuum radio emission was detected from the discs of either SBS 1129+576 or SBS 1129+577. The brightest continuum source in the field is 87GB 112918.9+574015 (which lies ~ 1.2 arcmin from the phase center) for which we measure a flux density of 130 ± 2 mJy. This source is coincident with the H I bridge (see Section 3.2), between the two galaxies. A search for H I absorption against this source (in the high-resolution data cube) gives a 3σ upper limit to the optical depth of 0.08 in the velocity range 1389–1706 km s⁻¹. If we take the H I column density to be 4.6×10^{20} atoms cm⁻² (i.e. as obtained from the 40-arcsec-resolution H I image at the position of the continuum source), this corresponds to a 3σ lower limit of 956 K on the spin temperature.

3.2 Line emission

The integrated H I emission map of the SBS 1129+576 field at an angular resolution of $\sim 42 \times \sim 40$ arcsec² is shown in Fig. 1. There is a clear bridge of emission connecting

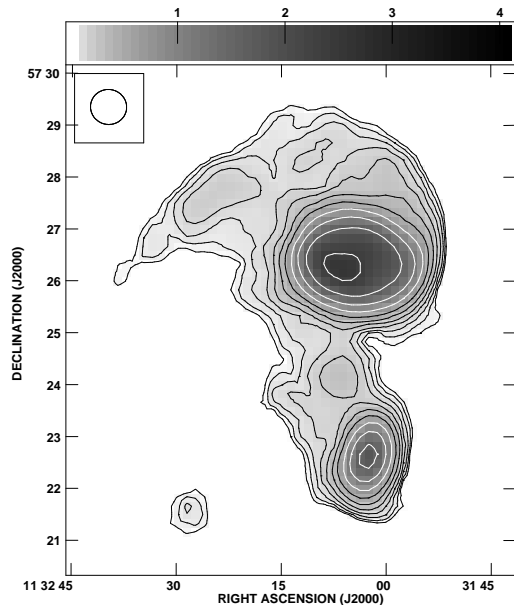


Figure 1. Integrated H I emission map of the SBS 1129+576 field in contours. The resolution is 42×40 arcsec² and the contours are at 3.0, 4.5, 6.8, 10.2, 15.2, 22.8, 34.3, 51.4, 77.1, 115.6 and 173.5×10^{19} atoms cm⁻². The same map is shown in grey-scale over column density range of 2.6×10^{19} – 2.7×10^{21} atoms cm⁻².

the two galaxies; SBS 1129+576 shows a hint of a tail to the south-west, while the outer gas in SBS 1129+577 is distorted into a strong one-armed spiral pattern. The total extent of H I emission from the two galaxies is 7.5×5.6 kpc². H I emission from a faint companion dwarf galaxy (SDSS J113227.68+572142.3) at an angular distance of 3.5 arcmin to the south-east of SBS 1129+576 is also detected.

Channel maps at the same resolution are shown in Fig. 2. A counterarm can be seen to develop on the north-western side of SBS 1129+577 at velocities ~ 1562 – 1576 km s⁻¹. The north-eastern part of this galaxy’s disc also shows H I extensions at a similar velocity range; this may be related to the H I in the bridge. At a velocity of 1592.7 km s⁻¹, these two arms are well developed and separated; however, at still larger velocities they appear to merge to form the one-armed spiral noted above. We detect H I emission from SDSS J113227.68+572142.3 in the velocity range 1526.0–1542.7 km s⁻¹. The emission is above the $\sim 3\sigma$ level in all the channels in this range, except for the channel at ~ 1529.3 km s⁻¹ in which it is $\sim 2\sigma$, and channel at 1539.3 km s⁻¹ in which there is no emission at this position.

The intensity-weighted velocity field (again at a resolution of ~ 40 arcsec) is shown in Fig. 3. The inner disc of SBS 1129+576 appears to have a velocity field consistent with solid body rotation, while the inner isovelocity contours of SBS 1129+577 are distorted. We discuss this further below. Smooth velocity gradients can also be noted in the bridge and the one-armed spiral. The continuity in the velocity field is consistent with that expected from a prograde encounter between both galaxies. As expected in

such an encounter, the rotational velocity gradient across SBS 1129+576 is in the same sense as that of the relative motion of SBS 1129+577. Similarly, the rotation velocity gradient across SBS 1129+577 is in the same sense as that of the relative motion of SBS 1129+576. The morphology of the system (i.e. well defined tidal tails and a bridge) is also consistent with such an encounter geometry (see e.g. Toomre & Toomre 1972). The morphology and kinematics of the system also strongly resemble those of H I 1225+01, which is also believed to be undergoing a prograde encounter (Chengalur, Giovanelli & Haynes 1995). Integrated spectra of SBS 1129+576, SBS 1129+577, the bridge emission and the dwarf companion are shown in Fig. 4, while the parameters derived from these spectra are given in Table 2. The sum of the H I flux from SBS 1129+576/SBS 1129+577 (i.e. 20.7 Jy km s⁻¹) is in good agreement with that measured by Thuan et al. (i.e. 21.6 ± 0.8 Jy km s⁻¹). We find $W_{50} \sim 85$ km s⁻¹ for SBS 1129+577 (which makes the dominant contribution to the total H I flux), again in good agreement with the value of 89 ± 2 km s⁻¹ given by Thuan et al. (1999). Position-velocity (P–V) diagrams along the major axis of SBS 1129+576 and SBS 1129+577 are shown in Fig. 5.

As discussed above (see also Fig. 1), at a resolution of ~ 40 arcsec SBS 1129+576 shows at most a hint of a counter tail. Higher-resolution ($\sim 17 \times 14$ arcsec² and 8×7 arcsec²) maps of the H I emission (overlaid on the Digitized Sky Survey II (DSS II) *B*-band optical image) from this galaxy are shown in Fig. 6. One can see that the H I distribution extends farther towards the south-east than towards the north-west. The integrated spectrum of the galaxy (Fig. 4) also shows more emission from gas at velocities corresponding to the southern half of the galaxy. In Fig. 6(a), one can also see that the contours near the southern tip of the optical disc extend towards the east. This is suggestive of a warp. In Fig. 6(b), one can see the extension more clearly, and also that the H I contours in the northern part of the galaxy have a corresponding (but smaller) bend towards the opposite direction, consistent with an integral-shaped warp of the H I disc. The gas in the northern end of the ‘warp’ blend into the bridge connecting the two galaxies.

The integrated 8×7 -arcsec²-resolution H I map of SBS 1129+577 (overlaid on the DSS II *B*-band optical emission) is shown in Fig. 7. The optical emission is shown in contours, whereas the H I emission is shown in grey-scale. The optical image shows a bar in the centre with a ring around it. The H I emission is broadly similar; the main differences being that the ring is more continuous in H I than in optical and that there is, in general, no clear correlation between the H I column density variations and the intensity of the optical emission in the bar.

The low-resolution velocity field of SBS 1129+577 (Fig. 3) suggests that the outer part of the gas disc is warped (compare e.g. with the velocity field of M51; Rots et al. 1990). Further, as noted above, the central regions show distorted isovelocity contours. The kinematical major axis and kinematical minor axis are not perpendicular to one another, as is typical for barred galaxies (e.g. NGC 5383; Sancisi, Allen and Sullivan 1979). The high-resolution (8×7 -arcsec²) velocity field (Fig. 8) also shows that the isovelocity contours are not parallel to each other within the bar. This is suggestive of an oval distortion in the potential with the gas moving along elliptical orbits (cf. Bosma 1981).

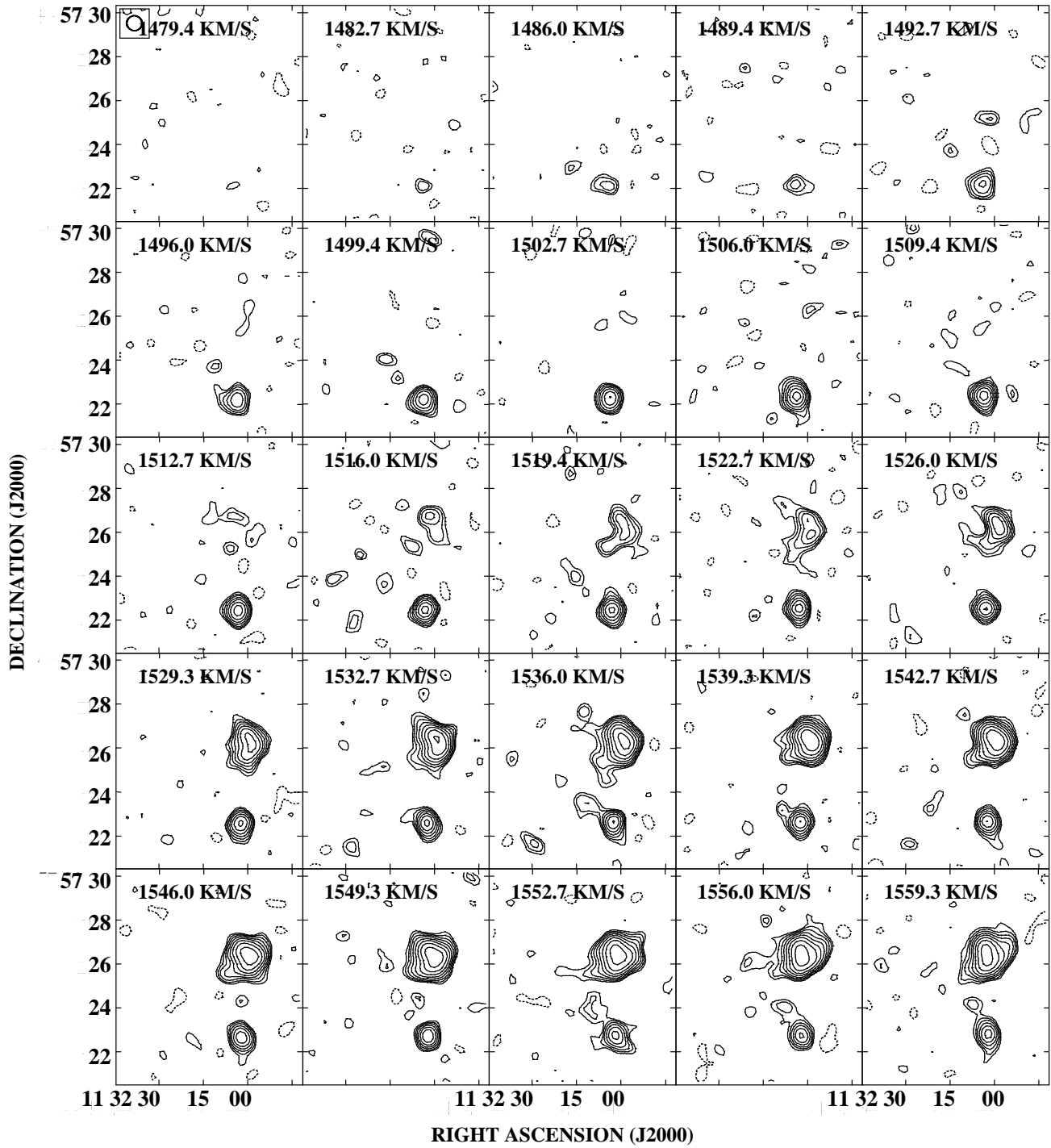


Figure 2. Channel maps for SBS 1129+576 and SBS 1129+577 at the resolution of 42×40 arcsec². The contour levels are at -3.2, 3.2, 4.5, 6.4, 9.1, 12.8, 18.1, 25.6, 36.2, 51.1 mJy Bm⁻¹.

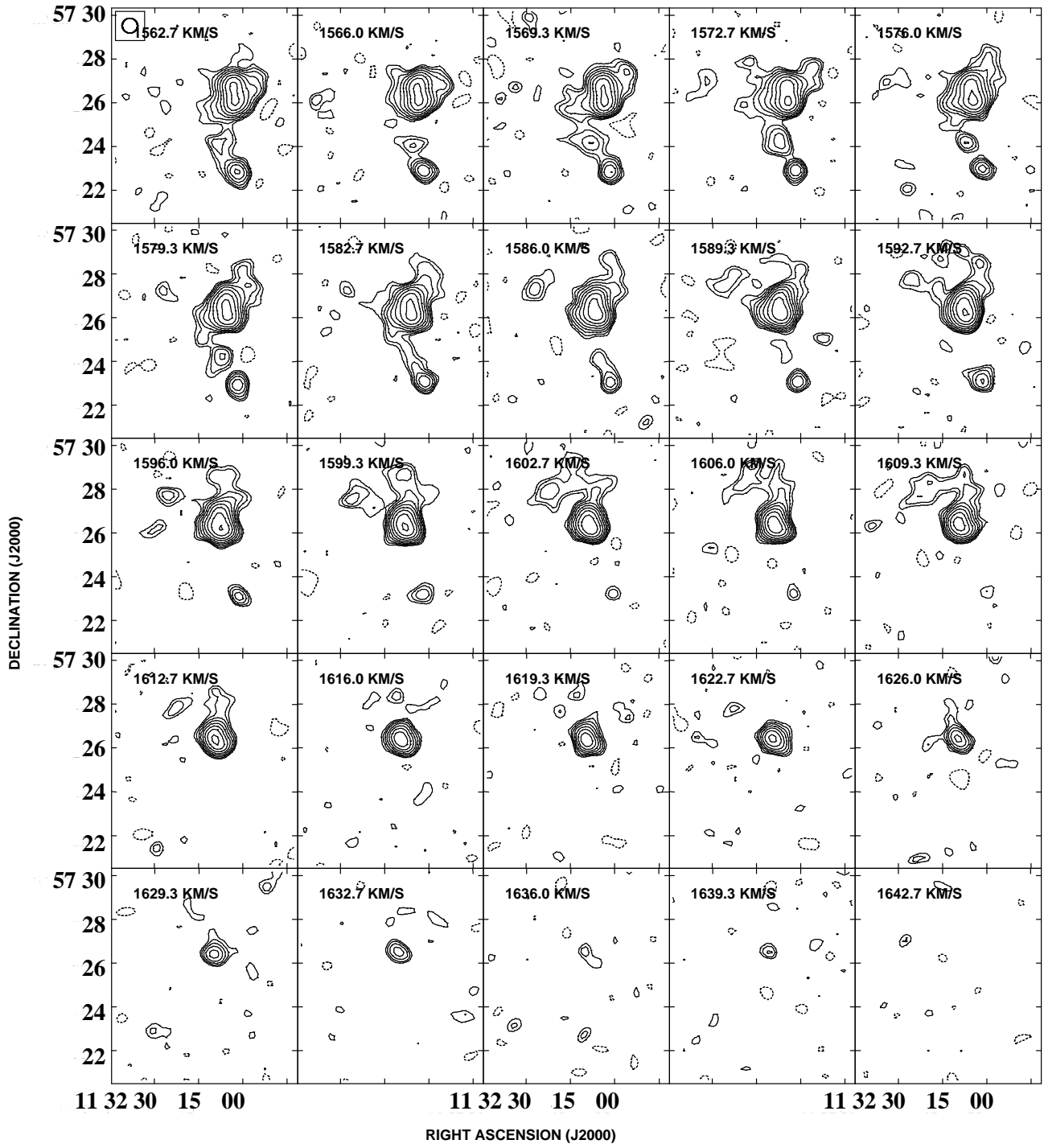


Figure 2. continued

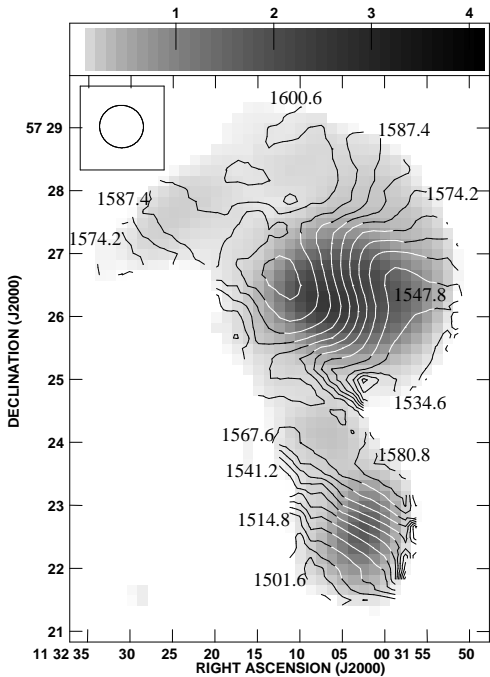


Figure 3. Intensity-weighted velocity field, made from 42×40 -arcsec² resolution data. The velocity contours are uniformly spaced with an interval of 6.6 km s^{-1} and range from 1495 to 1607 km s^{-1} . Integrated H I emission map is shown in grey-scale over column density range of 2.6×10^{19} – 2.7×10^{21} atoms cm^{-2} .

The velocity field of SBS 1129+576/577 system is very disturbed and we could not fit a rotation curve to the emission from the individual galaxies. We instead compute an indicative dynamical mass given by $M_{\text{ind}} = 2.3 \times 10^5 \times R_{\text{kpc}} \times V_{\text{kms}^{-1}}^2 M_{\odot}$. The maximum velocity seen in the P–V diagram in Fig. 5 is 60 km s^{-1} . Guseva et al. (2003) gave an axial ratio of 0.25 for this galaxy, which (assuming an intrinsic axial ratio of 0.25) implies that it is being viewed very close to edge-on. We hence take the inclination-corrected rotational velocity to be $\sim 60 \text{ km s}^{-1}$ at radius of $\sim 8.3 \text{ kpc}$, giving a dynamical mass of $M_{\text{dyn}} \sim 7.1 \times 10^9 M_{\odot}$ for SBS 1129+576. Similarly, from Fig. 5 the maximum radial velocity for SBS 1129+577 is 65 km s^{-1} . For this galaxy, the axial ratio listed in NASA/IPAC Extragalactic Database (NED) is ~ 0.77 , which corresponds to an inclination of $\sim 42^\circ$ (again for an intrinsic axial ratio of 0.25). The maximum rotational velocity is hence $\sim 88 \text{ km s}^{-1}$ at radius of $\sim 12 \text{ kpc}$. This gives an indicative dynamical mass of $M_{\text{dyn}} \sim 2.1 \times 10^{10} M_{\odot}$. The slices used while deriving P–V diagrams were along kinematic major axis for both the galaxies.

4 DISCUSSION

In Table 2, we summarise the main observational and derived parameters of SBS 1129+576 and its two companion galaxies. These two companion galaxies are sit-

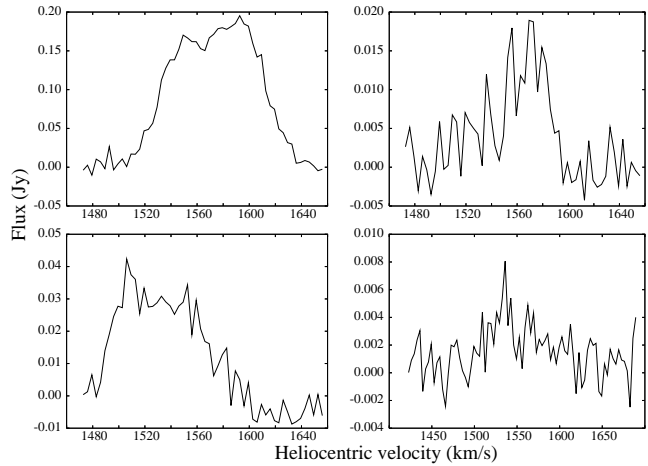


Figure 4. Integrated spectrum for the SBS 1129+577, bridge, SBS 1129+576 and companion dwarf made from the 42×40 -arcsec²-resolution data cube.

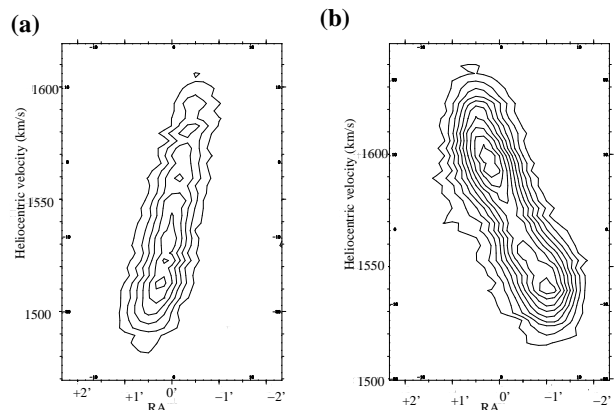


Figure 5. **a)** Major axis P–V diagram for SBS 1129+576. The contour levels are at 5, 10, 15, 20, 25, 29 mJy beam^{-1} . **b)** Major axis P–V diagram for SBS 1129+577. The contour levels are at 5, 10, 15, 20, 25, 30, 35, 40, 45, 49 mJy beam^{-1} .

uated $\sim 27 \text{ kpc}$ north (SBS 1129+577) and south-east (SDSS J113227.68+572142.3) of the XMD galaxy, respectively. The total projected size of this compact triplet is $\sim 43 \text{ kpc}$ and the range of their radial velocities is $\sim 70 \text{ km s}^{-1}$. The oxygen abundance in SBS 1129+577 is $12 + \log (\text{O}/\text{H}) = 7.94 \pm 0.08$ (based on Special Astrophysical Observatory (SAO) 6-m telescope observations; Pustilnik et al. 2006). This value is typical of BCGs with similar values of luminosity and suggests that it is an old galaxy. In contrast, SBS 1129+576 has $12 + \log (\text{O}/\text{H}) = 7.41 \pm 0.07$ (Guseva et al. 2003); there are only about a dozen or so known BCGs with metallicities comparable or lower than this. The third galaxy in the group, SDSS J113227.68+572142.3, has g and r magnitudes (as given in Sloan Digital Sky Survey (SDSS) Data Release 3 (DR3) data base; Abazajian et al. 2005) of 16.95 and 16.81 mag, respectively. Using the formulae in Smith et al. (2002), this translates to $B = 17.19 \text{ mag}$, $M_B = -14.8 \text{ mag}$. Similarly, translating the SDSS g and

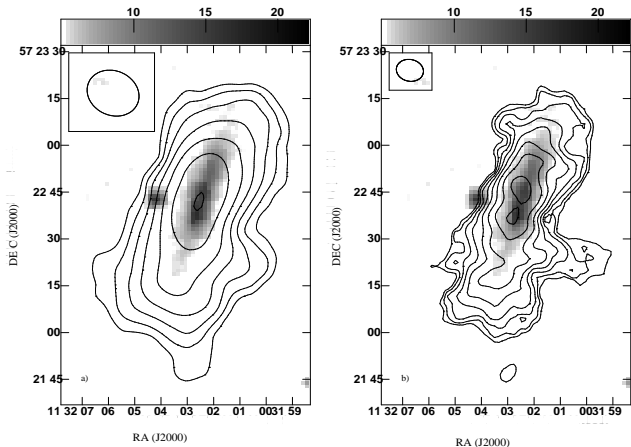


Figure 6. **a)** Integrated H I emission map (contours) of SBS 1129+576 at the resolution of 16×14 arcsec² overlaid on the optical DSS II *B*-band image (grey-scale in arbitrary units). The contour levels are at the column density of 3.4, 5.1, 7.7, 11.5, 17.3, 25.9, 38.9×10^{20} atoms cm⁻². **b)** Integrated H I emission map of SBS 1129+576 at the resolution of 8×7 arcsec² in contours overlaid on the optical *B*-band image in (grey-scale in arbitrary units). The contour levels are at the column densities of 3.4, 5.1, 7.7, 11.5, 17.3, 25.9, 38.9, 58.4×10^{20} atoms cm⁻².

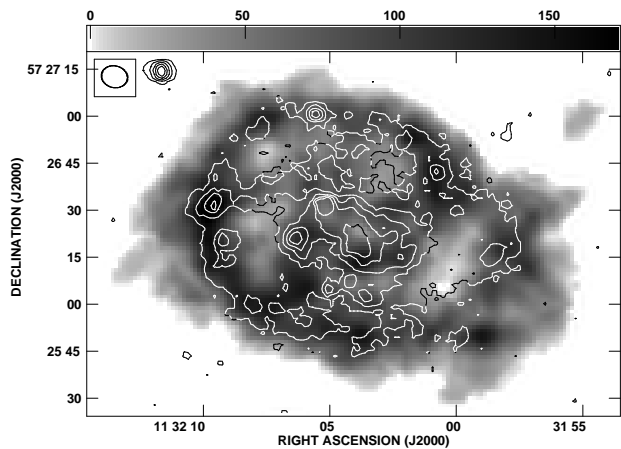


Figure 7. The DSS II optical blue band image (contours) overlaid on the integrated H I emission map of SBS 1129+577 (grey-scale over the range of H I column density from 0 to 3.6×10^{21} atoms cm⁻²) at a resolution of 8×7 arcsec⁻². The contours are logarithmically spaced and are in arbitrary units.

r magnitudes for SBS 1129+576 and SBS 1129+577 to *B* band, yields B_{tot} of 16.44 and 15.50 mag, respectively. Combining these with the H I masses derived in this paper gives M_{HI}/L_B of 2.1 and 3.8 (in solar units) for SBS 1129+576 and SBS 1129+577, respectively. Note that, in the value of M_{HI}/L_B for SBS 1129+576 we included the mass of gas in the bridge, assuming that it consists mainly of the gas pulled out of the less-massive galaxy. These values of M_{HI}/L_B are among the largest known for starburst galaxies and con-

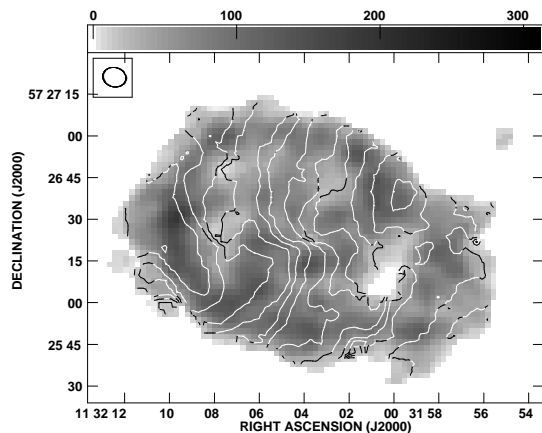


Figure 8. The velocity field of SBS 1129+577 at a resolution of 8×7 arcsec⁻² overlaid on the integrated H I emission (grey-scale over range of H I column density from 0 to 6.6×10^{21} atoms cm⁻²). The velocity contours are regularly spaced at an interval of 6.6 km s⁻¹ and range from 1528 km s⁻¹ to 1607 km s⁻¹.

firm that both these galaxies are gas-rich. In contrast, SDSS J113227.68+572142.3 is rather gas-poor, with $M_{\text{HI}}/L_B = 0.08$. The origin and evolution of such a system of quite different types of dwarf galaxies is probably worth a separate deeper study.

4.1 Star formation in SBS 1129+576, SBS 1129+577 and SDSS J113227.68+572142.3

As mentioned in Section 1, Guseva et al. (2003) presented detailed models of the star formation history of SBS 1129+576. Most of the current star formation is concentrated in two bright knots of emission (called regions 'a' and 'b' in Guseva et al. 2003). These two bright knots can also be seen in the broad-band optical image in Fig. 6, where it can also be seen that they coincide with peaks in the H I column density distribution. From the measured metallicity, the H α equivalent widths (EWs), and also assuming a standard Salpeter initial mass function (IMF), Guseva et al. (2003) estimate that these star-forming regions are very young, with ages $\lesssim 10$ Myr. Like in many other BCD galaxies, the current star formation activity in SBS 1129+576 appears to be occurring only above a critical H I threshold density. The observed peak H I column densities corresponding to H II regions 'a' and 'b' is $\sim 5.9 \times 10^{21}$ and $\sim 6.7 \times 10^{21}$ atoms cm⁻², respectively, at an angular resolution of 8 arcsec which corresponds to a linear resolution of 1.02 kpc at the assumed distance of 26.3 Mpc. These observed peak H I column densities correspond to deprojected values of the total gas density (i.e. including a 10 per cent contribution from He, we note that this is a slight overestimate of the He abundance in metal-poor galaxies) of $\sim 1.6 \times 10^{21}$ and $\sim 1.8 \times 10^{21}$ atoms cm⁻², similar to the values seen for other BCDs and dwarf irregular galaxies (e.g. Skillman 1987; Taylor et al. 1994).

Table 2. Main observational and derived parameters of the studied dwarf galaxies

Parameter	SBS 1129+576	SBS 1129+577	SDSS J113227+572142
α (J2000)	11 ^h 32 ^m 02 ^s .54	11 ^h 32 ^m 04 ^s .00	11 ^h 32 ^m 27 ^s .68
δ (J2000)	+57°22′45″.7	+57°26′20″.0	+57°21′42″.3
$\int f(v)dv$ (Jy km s ⁻¹)	3.9 ^a	16.7	0.07
V_{hel}^b (km s ⁻¹)	1506 ± 3.3	1575 ± 3.3	1540:
W_{50} (km s ⁻¹)	67 ± 3.3	85 ± 3.3	18:
m_B^c	16.44	15.50	17.19
M_B^d	-15.65	-16.59	-14.8
M_{HI} (10 ⁸ M _⊙)	6.3 ^a	27.0	0.11
M_{HI}/L_B^e	2.1 ^a	3.8	0.08
12 + log (O/H)	7.41 ± 0.07	7.94 ± 0.08	-

^a H I flux/mass of the bridge is included; ^b Heliocentric H I velocity;

^c Translated from SDSS *g* and *r* magnitudes;

^d Absolute blue magnitudes corrected for the MW extinction and D=26.3 Mpc;

^e In solar units.

The distribution of star-forming regions in SBS 1129+577 is more complicated. A long-slit spectroscopy of this galaxy was done by Pustilnik et al. (2006), using the SAO 6-m telescope. The slit was positioned at a position angle of 90° and passing through the brightest H II region A1 (J113206.5+572620; ~20 arcsec to the east of the centre of the main body seen in continuum). The peak H I column density at this position is 2.8×10^{21} atoms cm⁻² at an angular resolution of 8 arcsec. Besides this region, the star formation is also seen to take place in three more regions along the slit, namely A2, A3 and A4. A2 is ~20 arcsec to the east of A1, while A3 is ~35 arcsec to the west of A1. The H I column densities are 3.1×10^{21} and 2.4×10^{21} atoms cm⁻² at the positions of A2 and A3, respectively. A4, which is rather faint H II region near the centre of the galaxy, has an H I peak with column density of 3.2×10^{21} atoms cm⁻². We note that there are other brighter knots visible in the continuum optical image which also coincide with peaks in H I. For example, there is a bright optical condensation (J11329.9+572630) in the ring which coincides with the highest peak (4.1×10^{21} atoms cm⁻²) in the H I column density map. These too may be star-forming regions, but the confirmation by H α -imaging or spectroscopy is required. For the H II regions identified above via the long-slit spectroscopy, based on their measured EW(H β), we estimate ages of 4–8 Myr for the case of an instantaneous starburst model with the standard Salpeter IMF (Leitherer et al. 1999). The inclination-corrected total gas column densities for regions A1, A2, A3, and A4 are 2.3×10^{21} , 2.6×10^{21} , 2.0×10^{21} , and 2.6×10^{21} , respectively, all of which are similar to the canonical threshold density.

As mentioned above, SDSS J113227.68+572142.3 is gas-poor, with $M_{HI}/L_B = 0.08$. It does not appear to be strongly interacting with the other two galaxies and, in particular, there is no evidence for the exchange of matter between it and the two brighter galaxies of the group. The SAO 6-m telescope spectrum (unpublished) for this object as well as its SDSS DR3 spectrum show an H α emission line with EW = 28 Å, a faint [O III] λ 5007 line and Balmer absorption lines in blue. According to the Starburst-99 models of Leitherer et al. (1999), for an instantaneous starburst with

the metallicity $z = 0.0004$ and a standard Salpeter IMF, all of these features are consistent with a star formation episode with an age of ~20 Myr. This age is larger but comparable with that of the starbursts in SBS 1129+576 and SBS 1129+577. For SDSS J113227.68+572142.3, the peak H I column density (at a resolution of ~8 arcsec or 1 kpc) is $\sim 3.9 \times 10^{20}$ atoms cm⁻², corresponding to a deprojected total gas column density of $\sim 4.0 \times 10^{20}$ atoms cm⁻². This is a factor of ~2 below the nominal star formation threshold. We note that Begum et al. (2006) also found that star formation in very faint dwarf galaxies does occur at gas column densities approximately two times lower than the nominal threshold density. The size of the galaxy is comparable to our beam size, even at the highest resolution (i.e. ~8 arcsec). It is thus very likely that our observed peak column density is a severe underestimate of the true column density. It is possible that the star formation in SDSS J113227.68+572142.3 was triggered by the accretion of a small amount of gas onto a gas-poor (dwarf elliptical ?) progenitor. Deeper H I observations may help to confirm or rule out this hypothesis.

4.2 Comparison with other XMD galaxies

The SBS 1129+576/577 system is morphologically very similar to H I 1225+01 (Salzer 1992, Chengalur et al. 1995). Both systems consist of two components with a bridge between the two. In both systems, the southern component is almost edge-on, whereas the northern component is more face-on. The H I finger at the south-western edge of SBS 1129+576 is a countertail similar to that in the south-western component of H I 1225+01. The north-east clump of H I 1225+01 has a bar as SBS 1129+577 does have. Like in H I 1225+01, we assume that the H I in the bridge originates from the smaller galaxy in the pair. SBS 1129+576, like the south-western component in H I 1225+01, is on a prograde orbit. The H I masses of the less-massive components in both systems are similar (where we assume a distance of 15 Mpc to H I 1225+01). The ratio of the masses of the two components is, however, different, with a value of ~1:1.9 for H I 1225+01 and ~1:4.3 for SBS 1129+576/577. In computing these ratios, we assume that H I in the bridges originally belonged to less-massive components. The major difference

between the systems SBS 1129+576/577 and H I 1225+01 is that no optical counterpart has been found in south-west clump of H I 1225+01 to a limiting surface brightness of 27.0 V-mag arcsec⁻² (Salzer et al. 1991).

It is interesting to compare the environments of these systems. Salzer (1992) found that there is no dwarf galaxy within ~ 1 Mpc of H I 1225+01, while the nearest luminous galaxy is at ~ 1.2 Mpc from it (for an adopted distance of 15 Mpc). We re-examined the environment of H I 1225+01, using the data available in NED. We found that only one dwarf VCC 1208 (which is 124 arcmin north of H I 1225+01 and has $\delta V = 7$ km s⁻¹) lies within the ~ 1 Mpc limit given by Salzer (1992). This galaxy lies at a projected distance of 540 kpc (for $D = 15$ Mpc). The region around SBS 1129+576 was surveyed as a part of SDSS. Since there are no galaxies with 1300 km s⁻¹ $< V_{\text{hel}} < 1700$ km s⁻¹ within 30 arcmin (corresponding to the projected distance of 230 kpc), it seems to be an isolated group of dwarfs. There are several galaxies at the projected distances of 150–500 kpc with the velocities in the range ~ 1700 – 1800 km s⁻¹ (including a rather luminous SB(s)c galaxy NGC 3683, with $M_B = -19.6$ mag), but their radial velocities imply that all of them are more than ~ 2 Mpc away from the SBS 1129+576/577 system. There are four dwarf galaxies with radial velocities from 1450 to 1565 km s⁻¹ at the projected distances of ~ 350 – 400 kpc. The nearest luminous galaxy with close radial velocity is NGC 3619 ($M_B = -19.5$ mag) at ~ 0.8 Mpc. We conclude that both systems are at a distance of ~ 1 Mpc from the nearest luminous galaxies and at several hundred kpc from the nearest dwarf galaxy.

SBS 0335-052 (Pustilnik et al. 2001a) is another interesting object to compare to the SBS 1129+576/577 system. Both the components, SBS 0335-052 E and W, at a projected distance of 22 kpc (Pustilnik et al. 2001a) are candidate young galaxies (e.g. Izotov et al. 1997; Papaderos et al. 1998; Pustilnik, Pramskij & Kniazev 2004; Izotov, Thuan & Guseva 2005). The H I envelope surrounding these components is similar to the one seen in SBS 1129+576/577 system. Its total gas mass is comparable to that of SBS 1129+577 (i.e. $\sim 10^9 M_\odot$). The morphology and kinematics of SBS 0335-052 in H I and at other wavelengths suggest that the most plausible interpretation of this system is a merger. The progenitors are either extremely unevolved very gas-rich objects or protogalaxies. Their mutual tidal interaction has triggered the current bursts of star formation. The peak measured H I column densities are 1.0×10^{21} and 0.7×10^{21} atoms cm⁻² in the west and east components, respectively, at a linear resolution of 5.4×3.9 kpc. This system, however, seems to be not very isolated, lying at the outskirts of the loose group LGG 103. SBS 0335-052 is at a projected distance of ~ 150 kpc, and a velocity difference of ~ 120 km s⁻¹ from the luminous spiral NGC 1376.

Similarly, the current starburst in the low-metallicity galaxy HS 0822+3542 appears to be triggered by interaction with its companion SAO 0822+3545 (Pustilnik et al. 2003; Chengalur et al. 2006; but see Corbin et al. 2005 for an alternative interpretation). For I Zw 18, an XMD system with the second-lowest known metallicity, there is an extended H I distribution with four distinct components (van Zee et al. 1998), only two of which have optical counterparts.

Interpreting the observed configuration of SBS 1129+576 as the first close encounter (as is for the case of H I 1225+01), we would expect that the significant exchange of matter has not yet taken place. This is consistent with the large difference of metallicities (O/H differ by a factor of ~ 3 , or 0.5 dex). As noted by Pustilnik et al. (2004), in some of the probable XMD mergers, which are at more advanced stages, the differences in O/H in different components are significantly smaller. This is consistent with the gas exchange leading to a more homogeneous composition of ISM in the merging components towards the late stages of merger. In particular, for HS 0122+0743 (Pramskij et al. (2003); Pustilnik et al., in preparation), in which optical components are in contact, O/H differs by less than 0.1 dex. On the other hand, for SBS 0335-052 E and W, which seem to have their first close encounter the situation appears to be more complicated. While the galaxies are not expected to have exchanged much gas, their O/H differs by only 0.17 dex. This may be the result of the metal-enrichment by the first star formation episodes in both components leading to a typical value of $Z \sim 1/30 Z_\odot$ (Kunth & Sargent 1986). Summarising the comparison of SBS 1129+576 with several other XMD BCGs, we find that the tidal-interaction-triggered star formation is a common theme for all of them.

5 SUMMARY

We summarise our conclusions about this H I study of the metal-poor galaxy SBS 1129+576 and its immediate surroundings as follows:

(i) SBS 1129+576 is undergoing a strong interaction with the nearby dwarf galaxy SBS 1129+577. We assume that H I has been pulled out from it to form a bridge between the two galaxies. The mass of H I in the bridge is $2.1 \times 10^8 M_\odot$, roughly half the H I mass remaining in the disc of SBS 1129+576. The observed morphology of the system suggests that it is in a prograde orbit. The system is probably on its first encounter and no significant exchange of material has taken place yet. This is consistent with the very different ISM metallicities of the two systems. The enhanced star formation in these gas-rich galaxies (M_{HI}/L_B of 2.1 and 3.8) has very likely been triggered by mutual tidal interaction.

(ii) The two H I peaks in SBS 1129+576 are at face-on surface densities of $\sim 1.5 \times 10^{21}$ and $\sim 1.7 \times 10^{21}$ atoms cm⁻². These coincide with the positions of the two brightest H II regions, respectively. The face-on H I column density in H II regions identified in SBS 1129+577 using the slit spectroscopy is above $\sim 1.8 \times 10^{21}$ atoms cm⁻². This is similar in value to the threshold density for star formation seen in other BCGs.

(iii) SBS 1129+577 has a central bar with a ring surrounding it, while the outer gas has been distorted into a strong one-armed spiral pattern. These are also likely to be consequences of the tidal interaction.

(iv) The velocity field of SBS 1129+577 shows that the disc is warped in the outer region, while in the inner region the gas orbits appear to be non-circular, probably as a response to the potential of the central bar. There is a hint of an integral-shaped warp in the inner parts of disc of SBS 1129+576.

(v) The system has a third dwarf galaxy with H I mass of $1.1 \times 10^7 M_{\odot}$. It has an $M_{\text{HI}}/L_{\text{B}}$ value of 0.08, that is, much lower than those for its more-massive companions. While the optical spectrum of this galaxy indicates a recent star-formation episode (~ 20 Myr, comparable to that for starburst ages in SBS 1129+576 and SBS 1129+577), its low $M_{\text{HI}}/L_{\text{B}}$ suggests that it has had a very different evolutionary history. It is further unusual in having ongoing star formation, despite having a peak observed gas column density lower than the nominal threshold for star formation. We note, however, the true column density may be considerably higher than that derived from our comparatively low poor resolution maps.

(vi) The system SBS 1129+576/577 is similar in many aspects to two other well-known XMD systems. These are H I 1225+01 and SBS 0335-052 E and W, where the current star burst appears to have been triggered by tidal interaction.

Acknowledgment. SAP acknowledges the partial support from the Russian federal program 'Non-stationary phenomena in astronomy'. The authors acknowledge the spectral and photometric information from the SDSS data base, used for this study. The Sloan Digital Sky Survey (SDSS) is a joint project of the University of Chicago, Fermilab, the Institute for Advanced Study, the Japan Participation Group, the Johns Hopkins University, the Max-Planck-Institute for Astronomy (MPIA), the Max-Planck-Institute for Astrophysics (MPA), New Mexico State University, Princeton University, the United States Naval Observatory, and the University of Washington. Apache Point Observatory, site of the SDSS telescopes, is operated by the Astrophysical Research Consortium (ARC). We thank the GMRT staff for making these observations possible. The GMRT is run by the National Centre for Radio Astrophysics of the Tata Institute of Fundamental Research.

REFERENCES

- Abazajian, K. et al. 2005, *AJ*, 129, 1755
 Begum, A., Chengalur, J. N., Karachentsev, I. D., Kaisin, S. S., Sharina, M. E. 2006, *MNRAS*, 365, 1220
 Bosma, A. 1981, *AJ*, 86, 1825
 Chengalur, J.N., Giovanelli, R. & Haynes, M.P. 1995, *AJ*, 109, 2415
 Chengalur, J.N., Pustilnik S.A., Martin J.M., Kniazev A.Y. 2006, *MNRAS*, in press
 Corbin, M. R., Vacca, W.D., Hibbard, J.E., Somerville, R.S., & Windhorst, R.A. 2005, *ApJL*, 629, 89
 Guseva, N.G., Papaderos, P., Izotov, Y.I., Green, R.F., Fricke, K.J., Thuan, T.X. & Noeske, K.G. 2003, *A&A*, 407, 75
 Izotov, Y.I., Lipovetsky, V.A., Chaffee, F.H., Foltz, C.B., Guseva, N.G., Kniazev, A.Y. 1997, *ApJ*, 476, 698
 Izotov, Y.I., Thuan, T.X. & Guseva, N.G. 2005, *ApJ*, 632, 210
 Kunth, D., & Sargent, W.L.W. 1986, *ApJ*, 300, 496
 Kunth, D., & Östlin, G. 2000, *A&ARv*, 10, 1
 Leitherer, C. et al. 1999, *ApJS*, 123, 3
 Lipovetsky, V.A., Stepanian, J.A., Erastova, L.K., Shapovalova, A.I. 1988, *Afz*, 29, 548
 Markarian, B.E., & Stepanian, D.A. 1983, *Afz*, 19, 639
 Papaderos, P., Izotov, Y.I., Fricke, K.J., Thuan, T.X., & Guseva, N.G. 1998, *A&A*, 338, 43
 Petrosian, A., McLean, B., Allen, R.J., Leitherer, C., MacKenty, J., Panagia, N. 2002, *AJ*, 123, 2280
 Pramskij, A., Pustilnik, S., Kniazev, A., & Ugryumov, A., 2003, Preprint SAO No. 189
 Pustilnik S.A. & Martin J.-M. 2006, *A&A*, in press (Paper I)
 Pustilnik, S.A., Brinks, E., Thuan, T.X., Lipovetsky, V.A. & Izotov, Y.I. 2001, *AJ*, 121, 1413
 Pustilnik, S.A., Kniazev, A.Y., Lipovetsky, V.A., Ugryumov, A.V. 2001, *A&A*, 373, 24
 Pustilnik, S.A., Kniazev, A.Y., Pramskij, A.G., Ugryumov, A.V., Masegosa, J. 2003, *A&A*, 409, 917
 Pustilnik, S.A., Pramskij, A.G., Kniazev, A.Y. 2004, *A&A*, 425, 51
 Pustilnik, S., Kniazev, A., Pramskij, A., Ugryumov, A., Izotov, Y., & Green, R. 2006, *A&A* (submitted)
 Rots, A.H., Bosma, A., van der Hulst, J.M., Athanassoula, E., Crane, P.C. 1990, *AJ*, 100, 387
 Salzer, J.J. 1992, *AJ*, 103, 385
 Salzer, J.J., di Serego Alighieri, S., Matteucci, F., Giovanelli, R. & Haynes, M.P. 1991, *AJ*, 101, 1258
 Sancisi, R., Allen, R.J., Sullivan, W.T., III 1979, *A&A*, 78, 217
 Skillman, E.D. 1987, in Lonsdale Persson C.J., ed., *Star Formation in Galaxies*. NASA, Washington, p. 263
 Smith, J.A. et al. 2002, *AJ*, 123, 2121
 Taylor C.L., Brinks E., Pogge R.W., Skillman E.D. 1994, *AJ*, 107, 971
 Toomre A. and Toomre J. 1972, *ApJ*, 178, 623
 Thuan, T.X., Lipovetsky, V.A., Martin, J.M., & Pustilnik, S.A. 1999, *A&AS*, 139, 1
 van Zee, L., Westpfahl, D., Haynes, M.P., & Salzer, J. J. 1998, *AJ*, 115, 1000